KFUPM
Journal of Undergraduate Research International

Diamond Open Access 225
Article Physics

Charged-Particle Capture by a Schwarzschild Black Hole Equipped with a Dipole Magnetic Field

Aseel Bukhari and Abdallah Al Zahrani*

Cite https://doi.org/10.64589/juri/231594

Submitted: April 25, 2026 **Revised:** May 16, 2026 **Accepted:** May 21, 2026

ABSTRACT

This study investigates the equatorial capture of charged test particles by a Schwarzschild black hole immersed in an external dipole magnetic field generated by a current loop. In the standard Schwarzschild model, particle capture is governed by a single critical impact parameter. This study shows through analytical investigation and numerical solutions to differential equations of motion that a dipole magnetic field can qualitatively alter this behavior by producing two distinct maxima in the radial effective potential. When the azimuthal angular momentum and magnetic coupling parameter have the same sign, these maxima define the lower and upper critical impact parameters such that capture occurs only within a finite interval of the impact parameters. For the neutral Schwarzschild model, this bounded capture interval is absent; thus, this behavior constitutes a distinct feature of the magnetized system. The analysis conducted in this study further reveals that the magnetic field affects oppositely charged particles differently, thereby yielding selective charged-particle capture. This sign-dependent capture may contribute to the charge evolution of black holes in magnetized environments, a consideration which would culminate in more accurate models of particle capture by black holes in such astrophysical contexts.

Keywords: charged particles, capture cross-section, magnetized black holes, magnetic dipole field, critical impact parameter

1. INTRODUCTION

The accretion of matter by a black hole determines the evolution over time of important parameters, such as its mass, angular momentum, and possible electric charge; thus, this behavior provides valuable information on the black hole and its surrounding environment. A discussion of accretion naturally requires examination of black-hole capture cross-sections, which determine the range of incoming trajectories that yield capture.

For simplicity, black holes are often assumed to be non-magnetized and electrically neutral. This approximation is useful in many contexts, as astrophysical black holes are expected to carry only small electric charges. Herein, a "weak" electromagnetic field refers to a field sufficiently strong to affect the motion of a charged test particle but sufficiently weak that it does not modify the background spacetime geometry. The possible origins and relevance of weakly charged black holes have been discussed in previous studies [1–7]. Particular, the selective accretion of protons or electrons can influence the net charge of a black hole, whereas black-hole rotation in an external magnetic field may induce charge separation [1–7].

The accretion dynamics can also be strongly affected by the magnetic field surrounding the black hole [8–10]. External magnetic fields can modify charged-particle motion, accretion-disk dynamics, and the structures of effective potentials near compact objects. Notably, related idealized Schwarzschild models with external magnetic fields have also been applied to the dynamics of hot spots around Sgr A* [11]. These studies motivate the investigation of charged-particle capture in magnetized black-hole environments.

Capture cross-sections have been studied for several black-hole spacetimes and particle types. Specifically, the capture of massless and massive neutral particles by Schwarzschild black holes has been explored in standard treatments of black-hole physics [12]. Particularly, particle capture by Reissner–Nordström black holes was investigated by Zakharov [13], whereas Young analyzed capture by Kerr–Newman black holes, including the case of charged-particle motion under the Lorentz force [14]. Related studies have also examined null geodesics, ray tracing, lensing, shadows, trapped photons, and photon-region structure in higher-dimensional Schwarzschild–Tangherlini spacetimes [15–18], as well as massive-particle capture in such geometries [19]. Capture behavior in higher-dimensional rotating black-hole spacetimes has also been considered for the Myers–Perry metric [20].

Previous studies on particle capture by black holes primarily focused on cases in which the capture conditions were controlled by a single critical impact parameter. For neutral particles in Schwarzschild spacetime, spherical symmetry yields the standard disk-like capture condition. Extensions to the Reissner–Nordström, Kerr–Newman, and higher-dimensional black holes

Published under an exclusive license by KFUPM

modify the value of the critical impact parameter; however, discussion of the capture boundary in terms of a single limiting value is still typical.

This study investigates the equatorial capture of charged test particles by a Schwarzschild black hole immersed in an external dipole magnetic field, which is generated by a current loop. The electromagnetic field is treated as a test field; thus, it affects the charged-particle motion but does not modify the Schwarzschild background geometry. The present work differs from previous studies in that charged-particle capture occurs in a nonuniform external magnetic field generated by a current loop. This magnetic-field geometry changes the radial effective potential such that two relevant potential barriers can be produced in the equatorial plane. Consequently, the equatorial capture condition may be bounded by both the lower and upper critical impact parameters rather than by one parameter only. The results establish a new mechanism through which a magnetic field can selectively affect the capture of oppositely charged particles.

The general problem of charged-particle capture in a magnetized black-hole spacetime does not have a simple analytical solution, making numerical methods suitable for analysis. However, in the equatorial plane, this problem can be reduced to an effective-potential analysis that reveals important qualitative features.

The contributions of this study are twofold. First, the analysis reveals that the dipole magnetic field can produce two relevant maxima in the radial effective potential. Unlike the standard Schwarzschild case, in which the capture behavior is determined by a single critical impact parameter, in the magnetized case, lower and upper critical impact parameters can be produced, thereby yielding a bounded interval of impact parameters for equatorial capture. Second, the magnetic field affects oppositely charged particles differently; thus, a possible mechanism for selective charged-particle capture and, hence, charge evolution in magnetized black-hole environments is established.

The structure of this paper is as follows. In Section 2, the dynamics and capture of neutral particles by a Schwarzschild black hole are reviewed. Then, in Section 3, the charged-particle case in the external dipole magnetic field is examined and the equatorial capture behavior is analyzed for a range of magnetic coupling values. Note that the sign conventions of Misner et al.[21] are used, and geometrized units ($G = c = k_e = 1$), where k_e is Coulomb's constant, are adopted.

2. CAPTURE CROSS-SECTION OF NEUTRAL PARTICLES

2.1. Equations of Motion. Consider a neutral particle of mass m in the vicinity of a nonrotating black hole of mass M. The spacetime around this black hole is described by the Schwarzschild metric:

$$ds^2 = -f dt^2 + f^{-1}dr^2 + r^2 d\theta^2 + r^2 \sin^2\theta d\phi^2, \tag{1}$$

where $f = 1 - r_S/r$ and the Schwarzschild radius $r_S = 2M$. The spacetime admits four Killing vectors, two of which are expressed as follows:

$$\boldsymbol{\xi}_{(t)} = \xi^{\mu}_{(t)}\partial_{\mu} = \partial_t, \tag{2}$$

$$\boldsymbol{\xi}_{(\phi)} = \xi^{\mu}_{(\phi)}\partial_{\mu} = \partial_{\phi}. \tag{3}$$

These are associated with two commuting integrals of motion: the specific energy $\mathcal{E}$ and specific azimuthal angular momentum $\mathcal{L}$, which are given by

$$\mathcal{E} = -p_{\mu}\xi^{\mu}_{(t)}/m = \dot{t}f, \tag{4}$$

$$\mathcal{L} = p_{\mu}\xi^{\mu}_{(\phi)}/m = \dot{\phi}r^2\sin^2\theta. \tag{5}$$

Here, u^{μ} and $p^{\mu} = mu^{\mu}$ are the four-velocity and four-momentum of the particle, respectively. The overdot denotes the derivative with respect to the proper time of the particle. Using the normalization condition $u^{\mu}u_{\mu} = -1$, we can express the radial equation of motion in the equatorial plane as,

$$\dot{r}^2 = \mathcal{E}^2 - V(r), \tag{6}$$

where the effective potential $V(r)$ is given by,

$$V(r) = f\left(1 + \frac{\mathcal{L}^2}{r^2}\right). \tag{7}$$

The equations of motion can be expressed in dimensionless form by introducing the dimensionless quantities:

$$\sigma \equiv \frac{\tau}{r_S}, \rho \equiv \frac{r}{r_S}, \ell \equiv \mathcal{L}/r_S. \tag{8}$$

Hence, Eq. 7 becomes,

$$V(\rho) = \left(1 - \frac{1}{\rho}\right)\left(1 + \frac{\ell^2}{\rho^2}\right). \tag{9}$$

The effective potential $V(\rho)$ summarizes the competition between the gravitational attraction and the centrifugal barrier associated with the angular momentum. For particles arriving from infinity, capture occurs only if they have sufficient energy to surpass the maximum of $V(\rho)$. However, if the angular momentum is too large, the centrifugal barrier prevents the particles from reaching the black hole and the particles are scattered instead. Thus, the maximum of $V(\rho)$ determines the critical angular momentum ℓ_c and, equivalently, the critical impact parameter b_c separating capture from scattering.

2.2. Capture Cross-Section. The radial equation of motion of a neutral particle in dimensionless form reads,

$$\left(\frac{d\rho}{d\sigma}\right)^2 + V(\rho) = \mathcal{E}^2. \tag{10}$$

Capture is determined by the magnitude of the energy $\mathcal{E}$ in comparison to the maximum of $V(\rho)$. For a particle with a given specific $\mathcal{E}$, there exists a certain ℓ_c above which the particle is scattered and below which the particle is captured. The value of ℓ_c can be determined from the following conditions:

$$V(\rho) = \mathcal{E}^2, \qquad \frac{dV}{d\rho} = 0. \tag{11}$$

From Eq. 9, these two conditions yield,

$$\left(1 - \frac{1}{\rho}\right)\left(1 + \frac{\ell_c^2}{\rho^2}\right) = \mathcal{E}^2, \tag{12}$$

and

$$\rho^2 + \ell_c^2(3 - 2\rho) = 0, \tag{13}$$

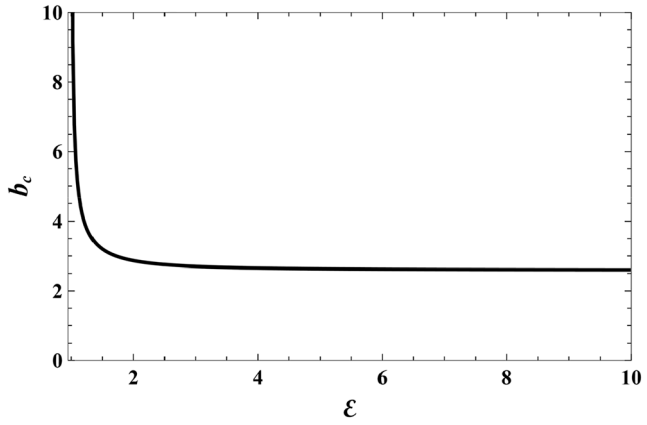

Figure 1. Critical impact parameter b_c for a neutral particle incident from infinity on a Schwarzschild black hole. Both b_c and the capture cross-section σ_{cap} diverge as $\mathcal{E}$ approaches 1 and approach their respective photon limits as $\mathcal{E}$ approaches infinity

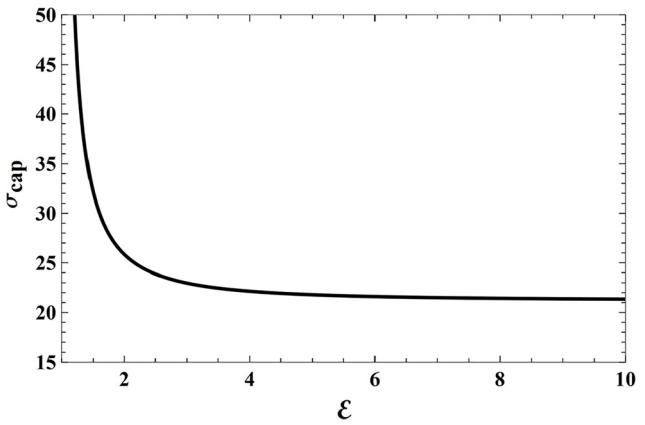

Figure 2. Capture cross-section σ_{cap} for the neutral-particle case. The general structure of the curve resembles that of b_c

respectively. Solving for ℓ_c^2 gives

$$\ell_c^2 = \frac{\left(9\mathcal{E}^2-8\right)^{3/2}\mathcal{E}+27\mathcal{E}^4-36\mathcal{E}^2+8}{8\left(\mathcal{E}^2-1\right)}. \tag{14}$$

The impact parameter b is defined as,

$$b = \frac{\ell}{p} = \frac{\ell}{\sqrt{\mathcal{E}^2-1}}, \tag{15}$$

where $p = \sqrt{(E^2-1)}$ is the magnitude of the particle's linear momentum per unit rest mass at infinity. Using Eq. 15, b_c can be expressed as,

$$b_c = \frac{\ell_c}{\sqrt{\mathcal{E}^2-1}} = \frac{\sqrt{\left(9\mathcal{E}^2-8\right)^{3/2}\mathcal{E}+27\mathcal{E}^4-36\mathcal{E}^2+8}}{\sqrt{8}\left(\mathcal{E}^2-1\right)}. \tag{16}$$

The capture cross-section is given by,

$$\sigma_{cap} = \pi b_c^2 = \pi\frac{\left(9\mathcal{E}^2-8\right)^{3/2}\mathcal{E}+27\mathcal{E}^4-36\mathcal{E}^2+8}{8\left(\mathcal{E}^2-1\right)^2}. \tag{17}$$

Figures 1 and 2 show how b_c and σ_{cap} vary with $\mathcal{E}$, respectively. In the ultra-relativistic particle case (i.e., $\mathcal{E} \gg 1$),

$$b_c = \frac{3\sqrt{3}}{2}+\frac{\sqrt{3}}{2\mathcal{E}^2}+O\left(\mathcal{E}^{-3}\right), \tag{18}$$

$$\sigma_{cap} = \pi\frac{27}{4}+\pi\frac{9}{2\mathcal{E}^2}+O\left(\mathcal{E}^{-3}\right), \tag{19}$$

which reduces to the photon capture cross-section as $\mathcal{E} \to \infty$.

3. CAPTURE CROSS-SECTION OF CHARGED PARTICLES FOR A MAGNETIZED BLACK HOLE

3.1. Equations of Motion. The electromagnetic potential A_μ that describes the dipole term of the magnetic field generated by an equatorial toroidal current loop of radius R around a Schwarzschild black hole is given by Petterson[22]:

$$A_\mu = \frac{1}{2}Br^2w\left(r\right)\sin^2\theta\delta_\mu^\phi, \tag{20}$$

where

$$w\left(r\right) = \begin{cases} 1, & 2M < r < R, \\ g(r) = (2M/r)(1+M/r) & r \geq R. \end{cases} \tag{21}$$

For a black hole immersed in an axially symmetric magnetic field of strength B[23], the inner potential reduces to the Wald solution while the outer potential has a richer current-loop structure. Here, we set $R = 3\ r_S = 2M$, corresponding to the Schwarzschild innermost stable circular orbit at $r = 6M$.

The Lie derivative of A_μ with respect to the two Killing vectors (Eqs. 2 and 3) vanishes everywhere:

$$\left(\mathcal{L}_\xi A\right)_\mu = \xi^\nu\partial_\nu A_\mu + A_\nu\partial_\mu\xi^\nu = 0. \tag{22}$$

For a charged particle of mass m and charge q, the generalized 4-momentum P_μ is given by,

$$P_\mu = mu_\mu + qA_\mu. \tag{23}$$

Then, the specific energy and specific azimuthal angular momentum definitions become,

$$\mathcal{E} = -P_\mu\xi_{(t)}^\mu/m = \dot{t}f, \tag{24}$$

$$\mathcal{L} = P_\mu\xi_{(\phi)}^\mu/m = \left[\dot{\phi}+\mathcal{B}w(r)\right]r^2\sin^2\theta, \tag{25}$$

where $\mathcal{B} = qB/\left(2m\right)$. Applying the normalization condition $u^\mu u_\mu = -1$, the equatorial radial equation of motion can be expressed as,

$$\dot{r}^2 = \mathcal{E}^2 - V(r), \tag{26}$$

with

$$V(r) = f\left[1+r^2\left(\frac{\mathcal{L}}{r^2}-\mathcal{B}w(r)\right)^2\right]. \tag{27}$$

Recast in dimensionless form, Eq. 27 becomes

$$V\left(\rho\right) = \left(1-\frac{1}{\rho}\right)\left[1+\rho^2\left(\frac{\ell}{\rho^2}-\beta w\left(\rho\right)\right)^2\right], \tag{28}$$

where $\beta = \mathcal{B}r_S$. There are two modes of radial motion, depending on the sign of $\ell\beta$. Without loss of generality, we set $\ell > 0$, consistent with the definition of b, and allow β to take both signs.

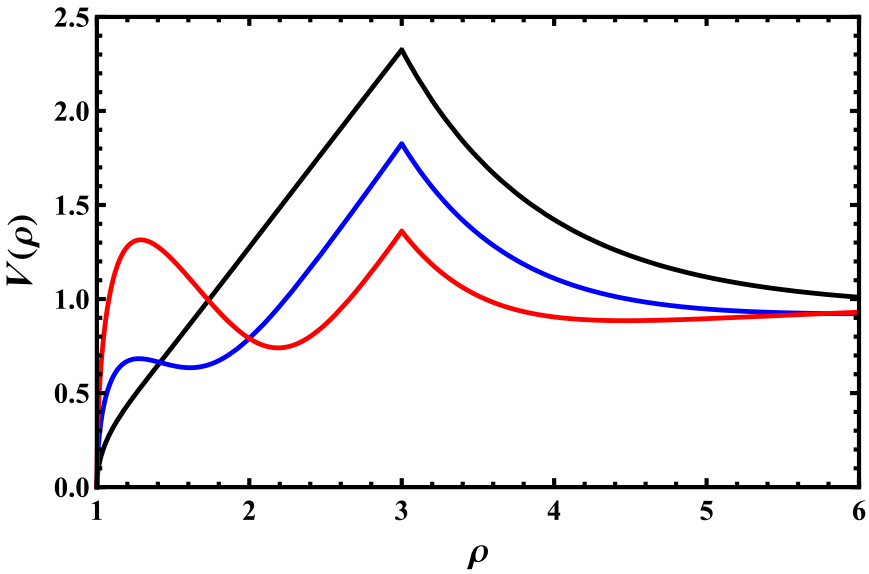

Figure 3. Radial effective potential for magnetic coupling parameter $\beta = 1$, current-loop radius $R = 3r_S = 6M$, and angular momentum $\ell = 1$ (black), 2 (blue), and 3 (red)

Compared with the neutral case, the charged-particle effective potential $V(\rho)$ contains an additional magnetic contribution through the combination $\ell/\rho^2 - \beta w(\rho)$ (Eq. 28). This term represents the coupling between the particle charge and external magnetic field. The sign of $\ell\beta$ is physically important because it determines whether the magnetic interaction enhances or opposes the angular part of the motion. Consequently, particles with opposite charges or those moving in opposite azimuthal directions relative to the magnetic field can experience different effective potentials and, therefore, different capture conditions.

3.2. Capture Cross-Section. Figure 3 shows the equatorial radial $V(\rho)$ for a positive magnetic coupling parameter β. In the neutral Schwarzschild case, the effective potential has a single relevant maximum, which provides a single b_c. In the magnetized case, the current-loop magnetic field introduces an additional structure to the potential. An inner maximum can appears inside the current loop and behaves similarly to the conventional Schwarzschild centrifugal barrier. A second feature appears near the loop radius, where the magnetic-field profile changes. For suitable values of $\ell\beta$, these two potential barriers define two critical impact parameters: b_{down} and b_{up}. In the equatorial plane, capture then occurs within a finite interval of impact parameters, $b_{down} < b < b_{up}$, rather than for all $b < b_c$.

When β is negative, two peaks can appear; however, both rise with ℓ and, therefore, correspond to an upper critical impact parameter b_{up} above which the particle is scattered.

Using the method of Sec. 2.2 and solving the resulting equations numerically, we find b_c for different β. Figure 4 plots b_c versus $\mathcal{E}$ for selected positive β. The blue (red) curves represent the upper (lower) critical impact parameter b_{up} (b_{down}). A charged particle is captured only when its b satisfies the condition $b_{down} < b < b_{up}$. Figure 5 plots b_c versus $\mathcal{E}$ for selected negative β. In this case, b_{down} does not exist. We also observe that b_{up} is not always smooth, because different maxima of $V(\rho)$ can determine its value.

These results are consistent with the known Schwarzschild limit. When β is small, the magnetic contribution to the effective potential weakens and b_c approaches the neutral-particle Schwarzschild result, as indicated by the dashed curve. This agreement provides a useful verification of the calculation. The main difference appears as the magnetic coupling increases: the current-loop magnetic field introduces an additional structure to the effective potential, which can generate a second critical impact parameter for one sign of $\ell\beta$. Therefore, the magnetic field not only shifts the Schwarzschild b_c, but also changes the qualitative form of the equatorial capture conditions.

Note that b_c in the magnetized case is calculated only for particles moving in the equatorial plane. Because an external magnetic field breaks the spherical symmetry, b_c generally depends on the direction from which the particle is fired relative to the equatorial plane, along with the direction of its linear momentum. Therefore, the full capture cross-section is not simply given by πb_c^2, as in the spherically symmetric Schwarzschild case. Nevertheless, the quantity constructed from the equatorial b_c is useful for comparing the capture behavior at different values of the magnetic coupling parameter. In what follows, this quantity is, therefore, interpreted as an equatorial capture measure rather than the full capture cross-section.

Figure 6 shows the equatorial capture measures corresponding to those shown in Fig. 4. For small β, the structure of the σ_{cap} curve is similar to that of the neutral-particle case. As β grows, a capture energy threshold appears; above this threshold, σ_{cap} grows rapidly to a maximum and then decreases until it approaches the neutral-particle value. Figure 7 shows the equatorial capture measures corresponding to those shown in Fig. 5. The structure of σ_{cap} is similar to that of the neutral-particle case and the magnetic field enlarges σ_{cap} over the range shown.

Therefore, the magnetic field can affect the charged-particle accretion selectively, according to the sign of qB (equivalently, the sign of β). Astrophysically, this sign dependence may bias the electron and proton accretion, thereby influencing the net charge

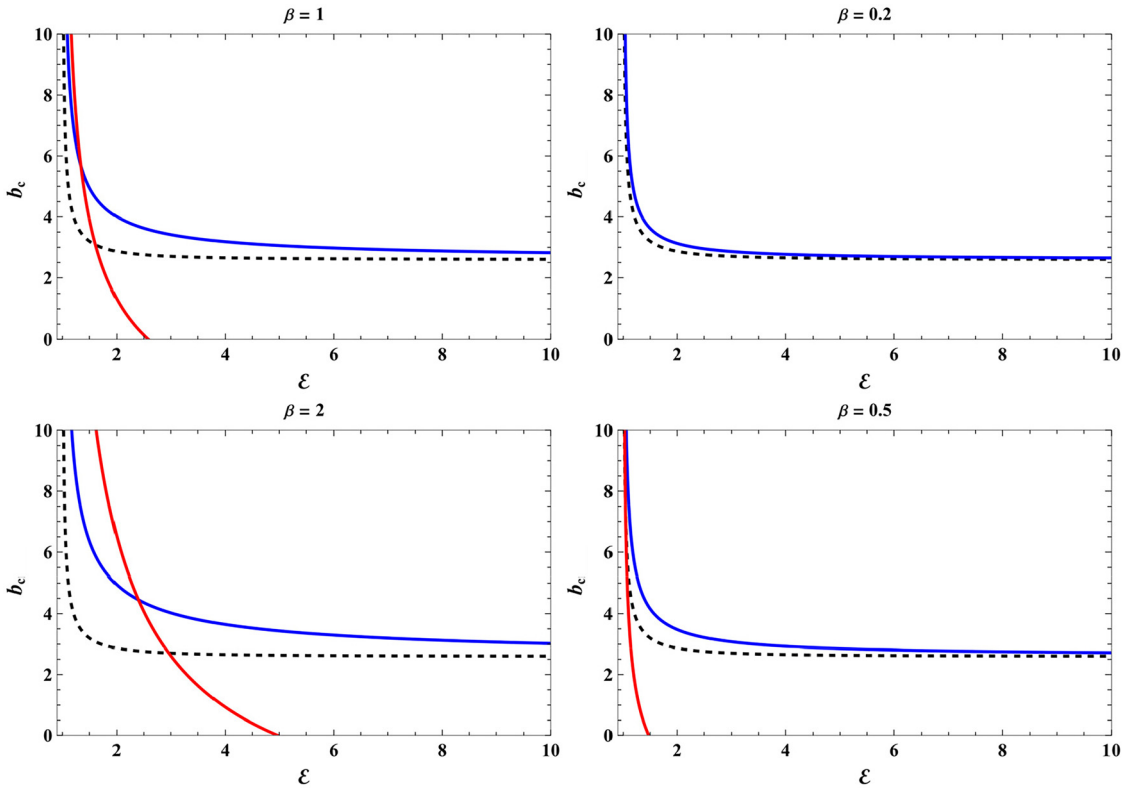

Figure 4. Critical impact parameters b_c for selected positive β. The dashed curve is the neutral-particle case. The blue (red) curve is the upper (lower) critical impact parameter $b_{up}(b_{down})$; capture occurs for $b_{down<b<b_{up}}$

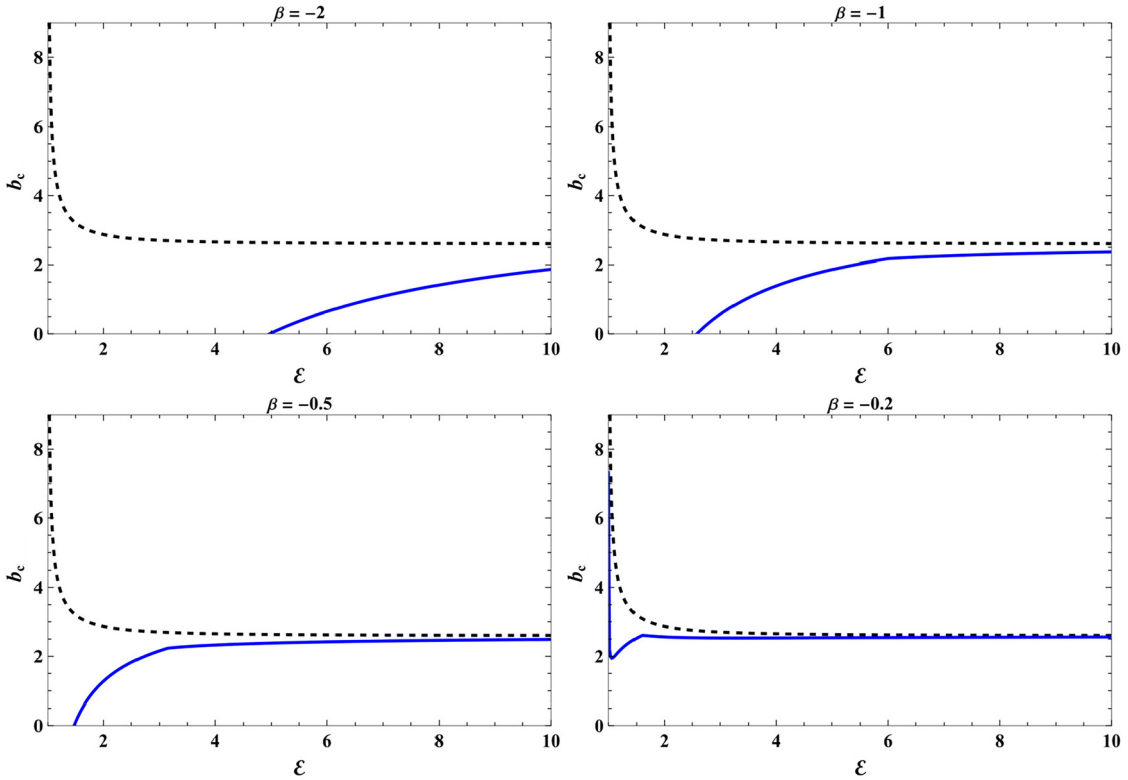

Figure 5. Critical impact parameter b_c for selected negative values of β. The dashed curve is the neutral-particle case. The blue curve indicates the upper critical impact parameter b_{up}, above which the particle is scattered

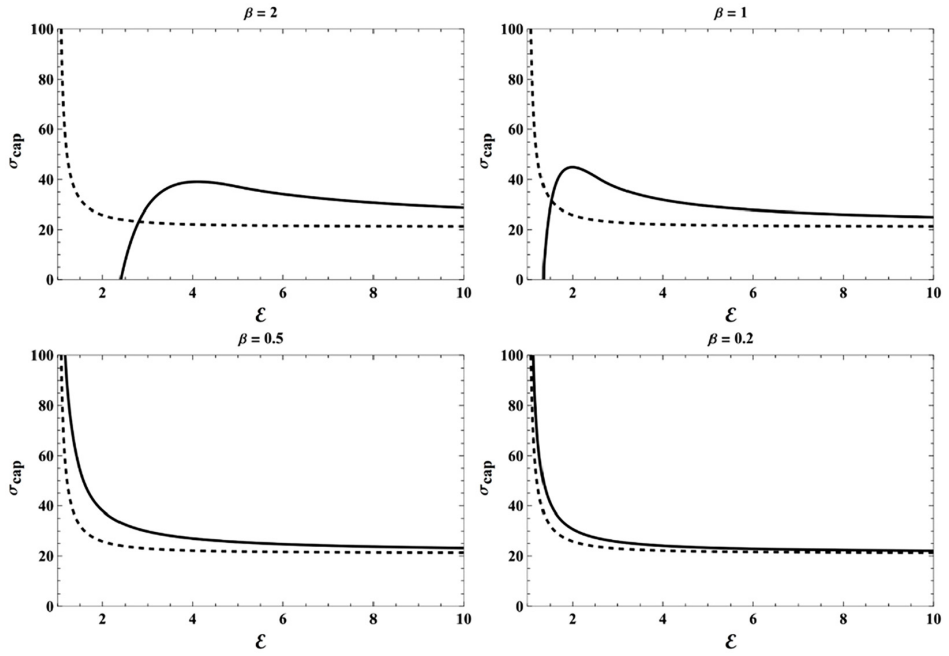

Figure 6. Equatorial capture measure σ_{cap} of charged particles for positive β. The dashed curve is the neutral-particle case

of the black hole or the surrounding plasma. Recall, however, that this study considers only the equatorial cross-section of the black hole, and a more comprehensive analysis of the capture measure across the entire sphere may reveal different global tendencies for the black hole.

4. CONCLUSIONS

This study examined the equatorial capture of charged test particles by a Schwarzschild black hole immersed in an external dipole magnetic field, where the magnetic field was generated by a current loop.

Based on the analytical results, the following key conclusions were drawn. At the weak-coupling limit, the results approach the familiar Schwarzschild behavior, in which the capture is governed by a single critical impact parameter. This agreement provides a useful consistency check for the analysis. The main finding is that the current-loop magnetic field can qualitatively modify the radial effective potential. For suitable magnetic-coupling

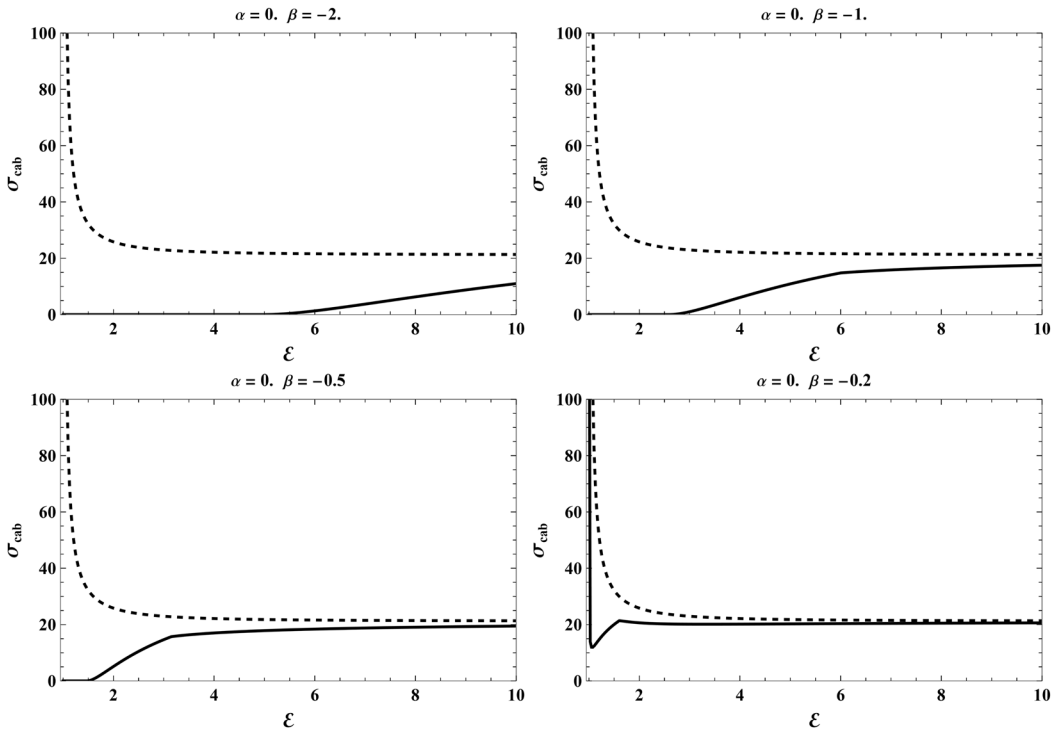

Figure 7. Equatorial capture measure σ_{cap} of charged particles for negative values of β. The dashed curve is the neutral-particle case

values, the effective potential can develop two relevant barriers in the equatorial plane. As a result, the equatorial capture condition can be bounded from below and above by two critical impact parameters, rather than being determined by a single upper critical value only. In the neutral Schwarzschild case, this behavior is absent. Further, this outcome demonstrates that the magnetic-field geometry can change not only the magnitude of the charged-particle capture but also its qualitative structure.

The analysis conducted in this study also revealed that the capture behavior depends on the sign of the magnetic coupling parameter relative to the azimuthal angular momentum. Therefore, oppositely charged particles experience different effective potentials and capture conditions under the same magnetic-field configuration. This sign-dependent behavior provides a possible mechanism for selective charged-particle accretion and may contribute to the charge evolution of black holes or their surrounding plasma in magnetized environments.

In conclusion, the immersion of a nonrotating black hole in a sufficiently strong magnetic field causes a charge-selective capture bias, a consideration relevant in modeling particle dynamics near black holes in such common astrophysical conditions. A natural extension of the present study is go beyond the equatorial approximation and investigate general three-dimensional charged-particle motion. This work is currently in progress. Such an extension would clarify the manner in which the equatorial features found in this study appear within the full capture region surrounding a magnetized black hole.

AFFILIATIONS AND AUTHOR DETAILS

Undergraduate Author

Aseel Bukhari – *Department of Electrical Engineering, King Fahd University of Petroleum & Minerals, Dhahran 31261, Saudi Arabia*; 0009-0007-8985-6233

Corresponding Author

Abdallah Al Zahrani – *Research Mentor, Department of Physics, King Fahd University of Petroleum & Minerals, Dhahran 31261, Saudi Arabia*; 0000-0002-5142-6904
Email: amz@kfupm.edu.sa

ACKNOWLEDGEMENTS

The authors acknowledge the support of the Undergraduate Research Office and the Department of Physics and Electrical Engineering at King Fahd University of Petroleum and Minerals.

REFERENCES

(1) Carter, B. Black hole equilibrium states. in *Black Holes* (eds DeWitt, C. & DeWitt, B. S.) 57–214 (Gordon and Breach, 1973).

(2) Zajaček, M., Tursunov, A., Eckart, A. & Britzen, S. On the charge of the Galactic centre black hole. *Mon. Not. R. Astron. Soc.* **480**, 4408–4423 (2018). doi:10.1093/mnras/sty218.

(3) Zajaček, M. *et al.* Constraining the charge of the Galactic centre black hole. *J. Phys. Conf. Ser.* **1258**, 012031 (2019). https://doi.org/10.1088/1742-6596/1258/1/012031.

(4) Zajaček, M. & Tursunov, A. Electric charge of black holes: Is it really always negligible? Preprint at https://arxiv.org/abs/1904.04654 (2019).

(5) Al Zahrani, A. M. Circular orbits of charged particles around a weakly charged and magnetized Schwarzschild black hole. *Phys. Rev. D* **103**, 084008 (2021). https://doi.org/10.1103/PhysRevD.103.084008

(6) Al Zahrani, A. M. Charged particle circular orbits around weakly charged and magnetized Kerr black holes. *Astrophys. J.* **937**, 50 (2022). https://doi.org/10.3847/1538-4357/ac8cf0

(7) Al Zahrani, A. M. & Al-Jama, A. Charged particles capture cross-section by a weakly charged Schwarzschild black hole. *Res. Astron. Astrophys.* **24**, 085012 (2024). https://doi.org/10.1088/1674-4527/ad63e6

(8) Stuchlík, Z., Kološ, M., Kovář, J., Slaný, P. & Tursunov, A. Influence of cosmic repulsion and magnetic fields on accretion disks rotating around Kerr black holes. *Universe* **6**, 26 (2020). https://doi.org/10.3390/universe6020026

(9) Chatterjee, K., Liska, M., Tchekhovskoy, A., Markoff, S. & Narayan, R. Extreme magnetic fields around black holes. *Astrophys. Space Sci. Proc.* **61**, 67–79 (2025). https://doi.org/10.1007/978-3-031-90186-7_6

(10) Abdurakhmonov, O. *et al.* Charged particles with magnetic dipole moment around magnetized Schwarzschild black holes surrounded by PFDM. *Chin. J. Phys.* **101**, 653–670 (2026). https://doi.org/10.1016/j.cjph.2026.02.004

(11) Rayimbaev, J., Ahmedov, B. & Stuchlík, Z. Particles with magnetic dipole moment orbiting magnetized Schwarzschild black holes: Applications to orbits of hot-spots around Sgr A*. *Phys. Dark Universe* **45**, 101516 (2024). https://doi.org/10.1016/j.dark.2024.101516

(12) Frolov, V. P. & Zelnikov, A. *Introduction to Black Hole Physics* (Oxford University Press, 2011). https://doi.org/10.1093/acprof:oso/9780199692293.001.0001

(13) Zakharov, A. F. Particle capture cross sections for a Reissner–Nordström black hole. *Class. Quantum Grav.* **11**, 1027–1033 (1994).

(14) Young, P. J. Capture of particles from plunge orbits by a black hole. *Phys. Rev. D* **14**, 3281–3289 (1976). https://doi.org/10.1103/PhysRevD.14.3281

(15) Connell, P. & Frolov, V. P. Ray-tracing in four and higher dimensional black holes: An analytical approximation. *Phys. Rev. D* **78**, 024032 (2008). https://doi.org/10.1103/PhysRevD.78.024032

(16) Tsukamoto, N., Kitamura, T., Nakajima, K. & Asada, H. Gravitational lensing in Tangherlini spacetime in the weak gravitational field and the strong gravitational field. *Phys. Rev. D* **90**, 064043 (2014). https://doi.org/10.1103/PhysRevD.90.064043

(17) Singh, B. P. & Ghosh, S. G. Shadow of Schwarzschild–Tangherlini black holes. *Ann. Phys.* **395**, 127–137 (2018). https://doi.org/10.1016/j.aop.2018.05.010

(18) Bugden, M. Trapped photons in Schwarzschild–Tangherlini spacetimes. *Class. Quantum Grav.* **37**, 015001 (2020). https://doi.org/10.1088/1361-6382/ab5493

(19) Ahmedov, B., Rahimov, O. & Toshmatov, B. Gravitational capture cross-section of particles by Schwarzschild–Tangherlini black holes. *Universe* **7**, 307 (2021). https://doi.org/10.3390/universe7080307

(20) Gooding, C. & Frolov, A. V. Five-dimensional black hole capture cross sections. *Phys. Rev. D* **77**, 104026 (2008). https://doi.org/10.1103/PhysRevD.77.104026

(21) Misner, C. W., Thorne, K. S. & Wheeler, J. A. *Gravitation* (W. H. Freeman, 1973).

(22) Petterson, J. A. Magnetic field of a current loop around a Schwarzschild black hole. *Phys. Rev. D* **10**, 3166–3170 (1974). https://doi.org/10.1103/PhysRevD.10.3166

(23) Wald, R. M. Black hole in a uniform magnetic field. *Phys. Rev. D* **10**, 1680–1685 (1974). https://doi.org/10.1103/PhysRevD.10.1680